Marine Target localization with passive GNSS-based multistatic radar: Experimental results

M.Antoniou, A.G. Stove, D. Tzagkas, M. Cherniakov
Dept. of Electronic, Electrical and Systems Engineering
University of Birmingham
Birmingham, United Kingdom
m.antoniou@bham.ac.uk

H. Ma
National Laboratory of Radar Signal Processing
Xidian University
Xi'an, China

***Abstract*—This paper considers passive multistatic radar with Global Navigation Satellite System (GNSS) transmissions (such as GPS and Galileo) for target localization. The paper briefly describes the appropriate signal processing algorithm, which is essentially a multi-lateration technique. However, particular emphasis is given on the experimental confirmation of the system, obtained through a proof-of-concept experimental campaign where a marine target was simultaneously detected by 11 transmitters and a single receiver.**

Keywords—passive radar; GNSS-based radar; multistatic radar

I. INTRODUCTION

Passive radar systems relying on Global Navigation Satellite Systems (GNSS) transmissions, such as GPS, GLONASS, Galileo and Beidou are finding increasing applications in radar and remote sensing through a number of different system topologies. For example, GNSS reflectometers (GNSS-R) for ocean remote sensing now form part of launched scientific missions such as the UK's TechDemoSat-1 [1] or CYGNSS [2]. In addition, GNSS-based Synthetic Aperture Radar (SAR) has been considered at length [3]-[5], showing the possibility to create ground imagery and detect temporal scene changes [6]-[7].

Recently, GNSS-based passive radar was brought forward for maritime surveillance purposes [8]-[9]. As a spaceborne system not originally intended for radar purposes, GNSS-based passive radar lacks the maritime target detection range offered by terrestrial transmitters, such as DVB-T [10] or FM

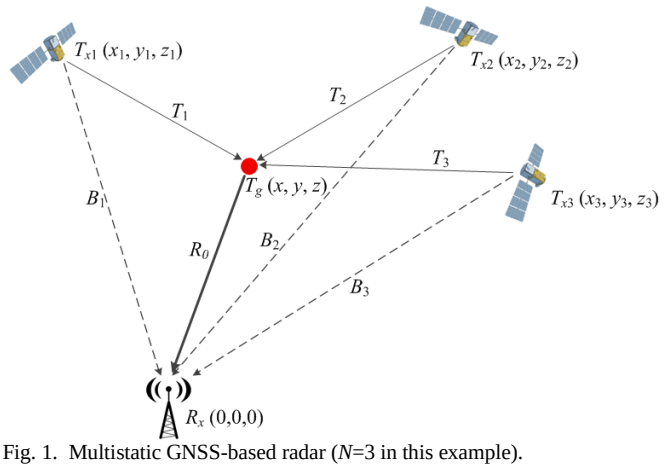

Fig. 1. Multistatic GNSS-based radar (N=3 in this example).

[11], however the global and persistent coverage offered by GNSS offers the capability to provide surveillance in areas where terrestrial illumination sources are not available, such as the open sea, and with an acceptable range resolution (up to15 m quasi-monostatic if the GPS L5 or Galileo E5a/b signals are used). However, the main highlight of this technology lies in the number of available satellites. At any time, each GNSS constellation guarantees a minimum of 4 satellites illuminating any point on Earth from different angles. More importantly, all these signals can be acquired by a single receiver and the modest power levels mean they can be separated at the signal processing level, without needing measures to reduce direct path interference, measures which are required in most of other passive radar concepts. This is because each GNSS constellation operates on a multiple access scheme (typically Code/Frequency Division Multiple Access, CDMA/FDMA) to discriminate signals from different satellites. This means that GNSS constellations can be inherently considered as multistatic radars with multiple, spatially diverse transmitters and a single receiver, which may introduce a number of advantages for remote sensing. For example, it has already been shown that this spatial diversity can be used to drastically improve spatial resolution in GNSS-based SAR images [12]. As a passive radar, and as the possibility to detect maritime targets in range and Doppler has already been shown [8], the next step is to begin considering benefits obtained from a multistatic operation. We begin by a study aimed to understand whether or not this kind of multistatic radar system can extract the location of a target in motion. In such a multistatic system, the fundamental theory is that it is possible to deduce the instantaneous location of a target if the bistatic ranges between each transmitter, the target and the receiver are known, which can be extracted by the relevant range-Doppler (RD) maps. In that respect, target localization was derived based on the Spherical Intersection (SX) method discussed in 0. More importantly, the derived algorithm was verified with experimental data from a proof-of-concept experimental campaign with a GNSS-based radar prototype in a real environment. In this experimental campaign, a large maritime target was detected by 11 GNSS satellites simultaneously, from all 3 major GNSS constellations. In addition, Automatic Identification System (AIS) data were available for both targets as ground truth. The remaining

content of this paper is arranged as follows: Section II briefly discusses the motivation for using GNSS-based radar for marine target localization. Section III derives the localization algorithm for GNSS-based multistatic radar. Next in Section IV, the proof of concept experimental setup and the relevant RD processing results are presented. Section V presents the experimental target localization results and compares them with ground truth.

II. GNSS-BASED RADAR FOR MARINE TARGET LOCALIZATION

Although other technologies exist for finding marine targets, passive radar has two great advantages for this application:

- it does not need a transmitting license and, similarly, it is easy to use multiple surveilance sites without mutual interference and
- it is covert, i. e. it is not possible to detect that is being used and it is therefore not possible to avoid surveillance.

By using a passive system, however, the performance of the system is dependent on the locations of the transmitters. In Western Europe the spacing of broadcast transmitters is often too sparse to enable a suitable choice of baselines to enable good localization and, invariably, they are located in land, limiting the range of baselines available for locating marine targets. GNSS systems, on the other hand provide global coverage with multiple transmitters which must be aligned in a favourable geometry to allow good location accuracy as navigation systems and hence will be well aligned to provide good location accuracy when used as illuminators for a passive radar.

One disadvantage of GNSS as an illuminator is that the illumination power is low. On the other hand, marine targets tend to be large and the system can integrate the power received from all the transmitters in view so that short-range coastal surveillance is practical.

Although systems using passive radars have intrinsic advantages as discussed above, for such systems to be used for marine surveillance they will still have to be cost-competitive with conventional marine radars. This means that they should be single-receiver, real aperture systems with wide-angle antennas, relying on multi-lateration alone, with several transmitters, to locate the targets. In fact such a receiver is potentially extremely low cost, allowing multiple installations to be used, reducing the maximum range at which any one sensor must work and thus further mitigating the disadvantage of the limited power density of the illuminators at the target.

III. TARGET LOCALIZATION WITH MULTISTATIC RADAR

A. Geometry and Problem Description

The system geometry in a local coordinate system is shown in Fig.1. The total number of satellites is represented by *N*. To analyze a multistatic passive radar with multiple transmitters and a single receiver, we can set the origin at the position of the receiver, so the location of the receiver is at (0,0,0). Since the receiver-to-target ranges are relatively short the ground or sea surface is modeled as a flat plane parallel to the (X,Y,0) plane. The coordinates of the target and satellites are denoted as:

$$T_g = \boldsymbol{x} = (x, y, z)^T, \quad (1)$$

and

$$T_{xi} = \boldsymbol{x_i} = (x_i, y_i, z_i)^T, \quad (2)$$

with the subscript *i* representing the satellite number.

Hence, the baseline between the *i*-th satellite and the receiver can be written as:

$$B_i = \|\boldsymbol{x_i}\| = \sqrt{x_i^2 + y_i^2 + z_i^2}, \quad (3)$$

the range between the *i*-th satellite and the target is:

$$T_i = \|\boldsymbol{x}_i - \boldsymbol{x}\| = \sqrt{(x_i - x)^2 + (y_i - y)^2 + (z_i - z)^2}, \quad (4)$$

and the range between the receiver and the target is:

$$R_0 = \|\boldsymbol{x}\| = \sqrt{x^2 + y^2 + z^2}. \quad (5)$$

When the target is illuminated by multiple satellites simultaneously, the radar can measure the appropriate bistatic target ranges and Doppler, by a basic RD processing described in [8]. As in the majority of passive/bistatic radar systems, bistatic range is measured based on the difference in time delay between a target echo and the direct signal from the transmitter to the receiver, while bistatic Doppler is measured by the relevant Doppler difference. Hence, at the output of the RD processor, for one particular target and particular satellite, the bistatic range may be written as:

$$r_i = T_i + R_0 - B_i. \quad (6)$$

The main idea of target localization is to apply multi-lateration techniques based on the difference of bistatic distances in (6).

On condition that all the relative bistatic ranges are measured accurately, we can lock the target onto its correct position. This can be solved by matrix method as following.

By rearranging (6), we have:

$$r_i + B_i - \sqrt{x^2 + y^2 + z^2} = \sqrt{(x_i - x)^2 + (y_i - y)^2 + (z_i - z)^2}. \quad (7)$$

After squaring the equation and a rearrangement, we obtain:

$$\left[B_i^2 - (r_i + B_i)^2\right] \Big/ 2 + (r_i + B_i) R_0 = \boldsymbol{x}^T \boldsymbol{x_i}, \quad (8)$$

which can be expressed as:

$$\boldsymbol{A}\boldsymbol{x} = \boldsymbol{K} + \boldsymbol{C}\|\boldsymbol{x}\|, \quad (9)$$

where $\boldsymbol{A}$ is the transmitter position matrix:

$$\boldsymbol{A} = \begin{bmatrix} \boldsymbol{x}_1 \\ \boldsymbol{x}_2 \\ \vdots \\ \boldsymbol{x}_N \end{bmatrix}_{N \times 3}. \quad (10)$$

$\boldsymbol{K}$ is constant vector denoted as:

$$\boldsymbol{K}=\frac{1}{2}\begin{bmatrix} B_1^2-(r_1+B_1)^2 \\ B_2^2-(r_2+B_2)^2 \\ \vdots \\ B_N^2-(r_N+B_N)^2 \end{bmatrix}_{N\times 1}, \quad (11)$$

and $\boldsymbol{C}$ is the sum of two constant vectors $\boldsymbol{R}$ and $\boldsymbol{B}$, respectively denoting the radar measured bistatic ranges and baselines:

$$\boldsymbol{C}=\boldsymbol{R}+\boldsymbol{B}=\begin{bmatrix} r_1 \\ r_2 \\ \vdots \\ r_N \end{bmatrix}_{N\times 1}+\begin{bmatrix} B_1 \\ B_2 \\ \vdots \\ B_N \end{bmatrix}_{N\times 1}. \quad (12)$$

As the only one unknown quantity in (9), the target position vector $\boldsymbol{x}$ can be given by the solution of (9).

It is well known that the most basic solutions to this problem, with only a small number of baselines can lead to 'ghost' solutions as well as the real one, due to the existence of the measurement error of bistatic ranges. However, when the number of satellites, i.e., in general, the number of bistatic range measurements, becomes greater than the dimensionality of the space (in our case, three dimensions) the ghost solutions vanish.

The discussion above addresses the case where a single target is present, and of course, when solving the multiple-target problem, we need to deal with more 'ghost' targets brought about by the solutions of different combinations of bistatic ranges corresponding to different targets. In the case discussed in this paper, the larger the number of GNSS transmitters, the greater the ability to distinguish between the real target and the unwanted ghosts directly and robustly since the more transmitters are available, the less likely it is that a 'ghost' will give a plausible false target position for a significant number of them.

B. General Solution Derivation

The left side of (9) conforms to the standard form of a linear equation set, however the right side contains a function of the unknown parameter, in the form of its determination as $\|\boldsymbol{x}\|$. For solving this equation set, we use the Spherical-Intersection (SX) method. Firstly, we ignore the existence of $\|\boldsymbol{x}\|$ in the right side of (9) and regard it as constant. Therefore, we can get a preliminary solution of $\boldsymbol{x}$ as:

$$\boldsymbol{x}=\left(\boldsymbol{A}^T\boldsymbol{A}\right)^{-1}\boldsymbol{A}^T\left(\boldsymbol{K}+\boldsymbol{C}\|\boldsymbol{x}\|\right). \quad (13)$$

We introduce two variables:

$$\boldsymbol{a}=\left(\boldsymbol{A}^T\boldsymbol{A}\right)^{-1}\boldsymbol{A}^T\boldsymbol{K}, \quad (14)$$

$$\boldsymbol{b}=\left(\boldsymbol{A}^T\boldsymbol{A}\right)^{-1}\boldsymbol{A}^T\boldsymbol{C}, \quad (15)$$

where $\boldsymbol{a}$ and $\boldsymbol{b}$ are vectors with size of 3×1. Then we have:

$$\boldsymbol{x}=\boldsymbol{a}+\boldsymbol{b}\|\boldsymbol{x}\|. \quad (16)$$

Substituting (16) into the equation of $\|\boldsymbol{x}\|^2=\boldsymbol{x}^T\boldsymbol{x}$, and after rearranging, we get the following quadratic equation for $\|\boldsymbol{x}\|$:

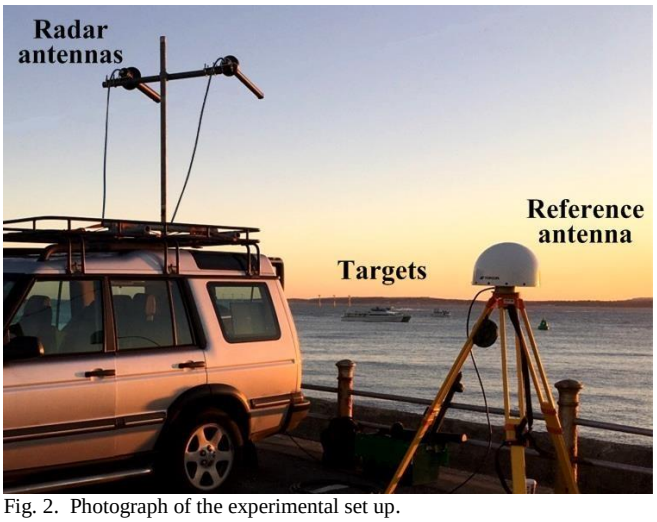

Fig. 2. Photograph of the experimental set up.

Fig. 3. Photograph of the target

$$\left(\boldsymbol{b}^T\boldsymbol{b}-1\right)\|\boldsymbol{x}\|^2+2\boldsymbol{a}^T\boldsymbol{b}\|\boldsymbol{x}\|+\boldsymbol{a}^T\boldsymbol{a}=0. \quad (17)$$

Hence, we can solve the receiver-to-target range as:

$$R_0=\|\boldsymbol{x}\|=\frac{-\boldsymbol{a}^T\boldsymbol{b}\mp\sqrt{\left(\boldsymbol{a}^T\boldsymbol{b}\right)^2-\left(\boldsymbol{b}^T\boldsymbol{b}-1\right)\boldsymbol{a}^T\boldsymbol{a}}}{\boldsymbol{b}^T\boldsymbol{b}-1}. \quad (18)$$

Then $\boldsymbol{x}$ can be obtained by substituting $\|\boldsymbol{x}\|$ into (17).

IV. Experimental Setup and Range-Doppler Maps

An experimental campaign was carried out to confirm the proposed technique. A passive receiver tuned to acquire GNSS signals was installed to the east of Portsmouth harbor in the UK. This was based on the SX3 receiver, manufactured by IFEN GmbH, a software-defined radio receiver designed for GNSS navigation, which we specifically customized for operation as a passive radar receiver. The receiver covered the following GNSS bands: GPS L1, GLONASS G1, and Galileo E5a and E5b. All four bands were recorded at a sampling rate of 20 MHz. Figure 2 shows a photograph of the experimental setup taken during the measurement.

The receiver was equipped with two channels, named as the reference and radar channels. The reference channel was connected to a low gain antenna to receive the direct signals from all satellites in its field of view. On the other hand, the radar channel used antennas pointed towards the target area.

As a proof-of-concept experiment, the receiver was based on the shore rather than in open sea and large targets moving relatively close to the receiver were sought to provide a sufficiently high SNR. At the time of measurement, a large target of opportunity (a commercial ferry, Fig.3) was presente with AIS equipped. The speed of the target was low as it entered port. This was the "Bretagne", with dimensions 158 m × 26 m.

Throughout the recording period the ferry was continuously illuminated by eleven satellites. The set includes two Galileo satellites, four Glonass satellites and six GPS satellites.

A. Range-Doppler Processing Results

Following data acquisition, a set of bistatic RD maps for the target were generated from each transmitter. The RD processor used has been discussed in detail in [8] so only its brief description will be provided here to avoid duplication.

Noting that since the satellites yield different bistatic ranges and Doppler frequencies, the RD processing needs to be applied to each individual satellite independently. Example RD maps for the target from three of the eleven different satellites belonging to different satellite systems (GPS, GLONASS, and Galileo) are shown in Fig.4 for brevity. Each RD map was computed using a 2.5 coherent integration time, with a non-coherent summation of four 2.5s RD maps. In all cases, the colourscale is in decibels, with 0 dB representing the highest intensity in each RD map, and a dynamic range artificially clipped to -25 dB. The highest intensity is at zero range and zero Doppler, which is the direct satellite signal received through the radar antenna sidelobes, as expected. Sidelobes of the direct signal are visible along zero Doppler. Returns at close ranges but spread in Doppler are attributed to sea clutter. Comparing the RD maps, it can be seen that the same target appears to be at a different bistatic range and Doppler for different satellites, as expected due to the difference in bistatic geometry and the difference in carrier frequencies across the GPS, GLONASS and Galileo bands used. It should be stated here that in an operational case where multiple targets are simultaneously detected, it may be a formidable task to associate multiple bistatic detections to a particular target in question. However, this is a subject for further study which is beyond the scope of this paper. Looking at RD maps of the same target, it is also interesting to mention that the relative intensity of the target and clutter can vary considerably, which may introduce benefits for target detection in the future.

One of the most obvious differences across RD maps obtained by different satellite constellations is the available range resolution, since the signal bandwidths used are substantially different. These also cause return signal intensities to vary. For example, the GPS L1 signal with a 1 MHz bandwidth gives a 150 m range resolution, which is comparable to the dimensions of the target, whereas for Galileo E5a with a 10 MHz bandwidth a range resolution cell corresponds to just a portion of a target.

V. Experimental Multi-static Target Localization

Based on the measured bistatic ranges seen from multiple satellites at the RD maps, we can localize the target at any particular time. By applying the method in Section III, we obtained the target localization results for the target with increasing numbers of satellites up to the maximum of 11. The results are illustrated in Fig.5. These figures are 'North Up,' so East is to the right. In these figures, the red '*' marks show all the obtained target location with a step of 1 s using a certain number of satellites. The blue continuous lines are the AIS track serving as the ground truth.

Comparing the results in the figure it can be seen that the proposed approach can correctly localise the target. It also shows that as the number of satellites increases, the target is localised more accurately, as expected. To get a numerical understanding of the improvement of target localization performance as the number of satellites increases, we calculated the Root Mean Square (RMS) of the detected track deviations in cases of different numbers of satellites, using the target's AIS track as the reference. The results are shown in Table I. The table shows that as the number of satellites increases, localization accuracy also increases, but after 6

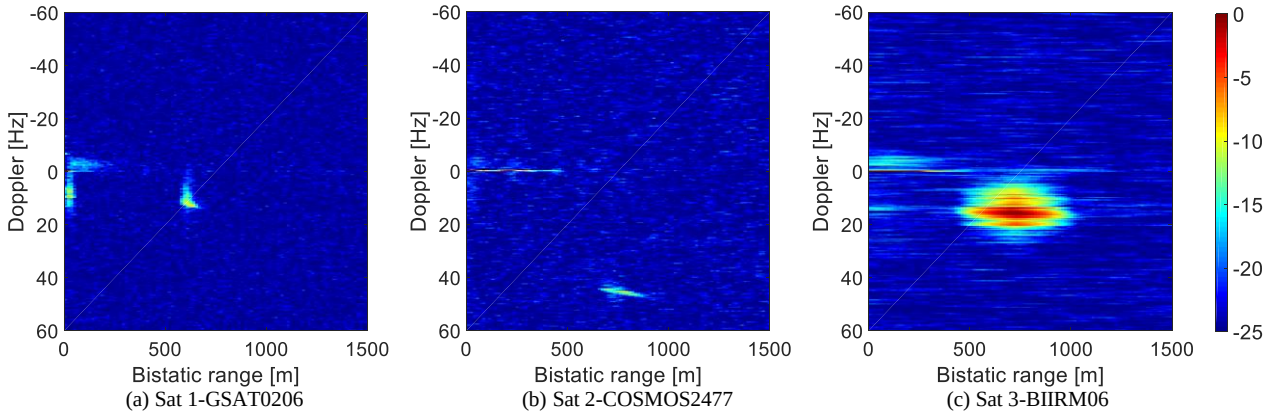

Fig. 4. Example RD maps of target from a (a) Galileo, (b) GLONASS, (c) GPS satellite.

satellites the improvement is not as noticeable.

TABLE I. RMS LOCALIZATION ACCURACY

No. of satellites	Localization accuracy (m)
3	68
6	50
8	49
11	48

VI. CONCLUSIONS

This paper has shown that passive multi-static radar based on GNSS transmissions can be used to determine the instantaneous position of a target. This can be achieved by exploiting the spatial diversity provided by GNSS constellations while using a single receiver. Algebraic equations have been derived in order to do so. Theoretical results have been supported by a proof of concept experimental campaign with maritime targets. In this campaign, a target was detected by 11 different GNSS satellite transmitters simultaneously, which to the authors' knowledge is the first experimental measurement of this kind at such a scale. Theory and results obtained here can be extended from passive multi-static GNSS-based radar to any multi-static radar, active or passive.

It is important to demonstrate that it is possible to go from the bistatic range-Doppler plots obtainable from a single transmitter to actually locate the target. We have shown this, but there are surprisingly few other descriptions of passive radars which show that this step can actually be achieved in practice. At the same time, it brings GNSS-based radar experimental test beds forward as a means of testing general multi-static radar theory, due to the relative ease of experimentation with GNSS as opposed to building a dedicated multi-static system with a large number of transmitters and receivers

Now that the capability in localizing objects with this system has been confirmed, the next stage in research is to investigate how multi-static radar systems can be used to indicate the kinematic state of a target.

ACKNOWLEDGMENT

Work on the conversion of the SX3 to a passive radar receiver was supported under a contract of the European Space Agency in the frame of the Announcement of Opportunities on GNSS Science and Innovative Technology within the European GNSS Evolutions Programme (EGEP ID 89).

REFERENCES

[1] A. Alonso Arroyo, V. U. Zavorotny, A. Camps, "Sea ice detection using GNSS-R data from UK TDS-1", IGARSS 2016, pp. 2001-200, July 2016.

[2] M.P. Clarizia, C. S. Ruf, "Wind speed retrieval algorithm for the CYGNSS mission", IEEE Trans. Geosc. Rem. Sens., vol. 54, no. 8, pp. 4419-4432, August 2018.

[3] M. Cherniakov (ed.) *Bistatic radar- emergine technology*, Chichester: Wiley, 2007, Wiley, ISBN 978-0-470-02630-4

[4] M.Antoniou and M. Cherniakov, "GNSS-based bistatic SAR: A signal processing view," *EURASIP Journal on Advances in Signal Processing*, no.1, pp. 1-16, Mar. 2013.

[5] M. Antoniou and M. Cherniakov, "GNSS-based radar", in R. Klemm (ed.) *Novel Radar Techniques and Applications*, SciTech Publishing, 2018, ISBN 978-1-61353-225-6.

[6] F. Liu, M. Antoniou, Z. Zeng, M. Cherniakov, "Coherent change detection using passive GNSS-based BSAR: experimental proof of concept," *IEEE Trans. Geosci. Remote Sens.*, vol. 51, no. 8, pp. 4544-4555, Aug. 2013.

[7] D. Tzagkas, M. Antoniou, M. Cherniakov, "Coherent change detection experiments with GNSS-based bistatic SAR", EuRad 2016, pp. 262-265, October 2016.

[8] H. Ma, M. Antoniou, D. Pastina, F. Santi, F. Pieralice, M. Bucciarelli, M. Cherniakov, "Maritime moving target indication using passive GNSS-based bistatic radar", IEEE Trans. Aer. Elec. Syst., in press.

[9] H. Ma, M. Antoniou, M. Cherniakov, D. Pastina, F. Santi, F. Pieralice, M. Bucciarelli, "Maritime target detection using GNSS-based radar: Experimental proof of concept", IEEE Radar Conference 2017, pp. 464-469.

[10] M. Conti, F. Berizzi, M. Martorella, E. DalleMese, D. Petri, A. Capria, "High range resolution multichannel DVB-T passive radar," *IEEE Aerosp. Electron. Syst. Mag.*, vol. 27, no. 10, pp. 37-42, Oct. 2012.

[11] F. Colone, D. W. O'Hagan, P. Lombardo, C. J. Baker, "A multistage processing algorithm for disturbance removal and target detection in passive bistatic radar," IEEE Trans. Aerosp. Electron. Syst.vol. 45, no. 2, pp. 698-722, Apr. 2009.

[12] F. Santi, M. Bucciarelli, D. Pastina, M. Antoniou, M. Cherniakov, "Spatial resolution improvement in GNSS-based SAR using multistatic acquisitions and feature extraction," *IEEE Trans. Geosci. Remote Sens.*, vol. 54, no. 10, pp. 6217-6231, October 2016.

[13] G. Mellen, M. Pachter, J. Raquet, "Closed-form solution for determining emitter location using time difference of arrival measurements," *IEEE Trans. Aerosp. Electron. Syst.*, vol. 39, no.3, pp. 1056-1058, Jul. 2003.

[14] D. W. O'Hagan. A. Capria, D. Petri, V. Kubica, M. Greco F. Berizzi and A. G. Stove, "Passive bistatic radar (PBR) for harbour protection applications," proc. IEEE Radar Conf. 2012, pp 446-50.

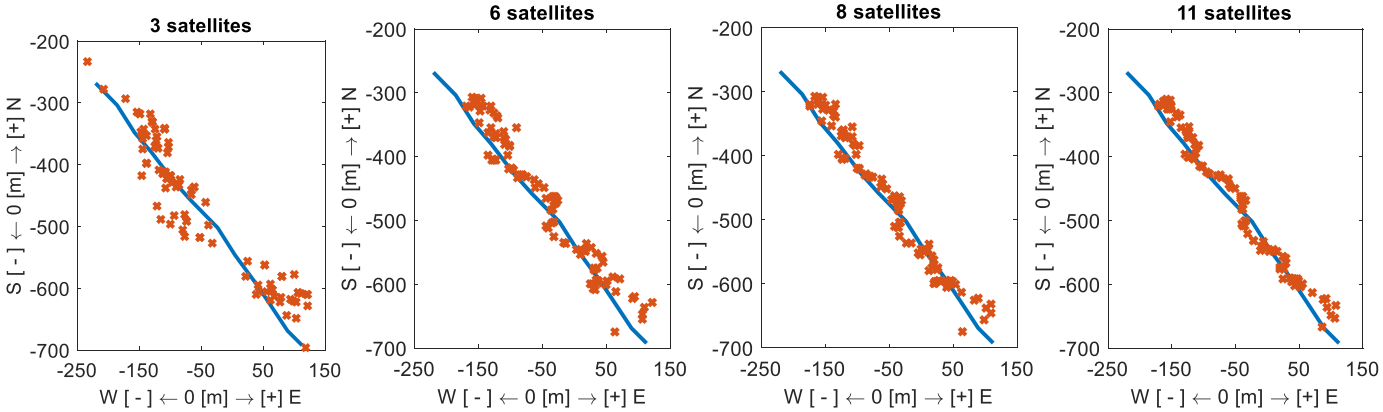

Fig. 5. Target location vs no. of satellites